chemosensors

MDPI

Article

Development of an Online Instrument for Continuous Gaseous PAH Quantification: Laboratory Evaluation and Comparison with The Offline Reference UHPLC-Fluorescence Method

Joana Vaz-Ramos [1,2], Mathilde Mascles [3], Anaïs Becker [1], Damien Bourgain [3], Audrey Grandjean [1,3], Sylvie Bégin-Colin [2], Franck Amiet [3], Damien Bazin [3] and Stéphane Le Calvé [1,*]

1 Institut de Chimie et Procédés Pour l'Energie, l'Environnement et la Santé (ICPEES), UMR-7515 CNRS-Université de Strasbourg, 25 Rue Becquerel, 67087 Strasbourg, France; joana.vazramos@ipcms.unistra.fr (J.V.-R.); ana.becker@unistra.fr (A.B.); audrey.grandjean@chromatotec.com (A.G.)
2 Institut de Physique et Chimie des Matériaux de Strasbourg (IPCMS), UMR-7504 CNRS-Université de Strasbourg, 23 Rue du Loess, 67034 Strasbourg, France; sylvie.begin@unistra.fr
3 Chromatotec, 15 Rue d'Artiguelongue, 33240 Saint-Antoine, France; mathilde.mascles@chromatotec.com (M.M.); damien.bourgain@chromatotec.com (D.B.); franck.amiet@chromatotec.com (F.A.); damien.bazin@chromatotec.com (D.B.)
* Correspondence: slecalve@unistra.fr

Abstract: Polycyclic aromatic hydrocarbons (PAHs) are widespread environmental contaminants formed during incomplete combustion or pyrolysis of organic material. The reliable quantification of PAH in airborne samples is still difficult, costly, and time-consuming due to the use of offline techniques, including long sampling on filters/adsorbents, laboratory extraction, purification, and concentration steps before analysis. To tackle these drawbacks, this work focused on the development of a fully automatic gas chromatograph (GC) equipped with a flame ionization detector (FID) and a sample preconcentration unit (PC) for gas sampling. This instrument was validated under laboratory-controlled conditions in the range 0–10 ng for 18 PAH. The chromatographic separation was rather satisfactory except for two PAH pairs, which were quantified together. For all compounds, the peak areas increased perfectly with the gaseous PAH concentration ($R^2 > 0.98$), without any significant memory effect between two consecutive analyses. Considering a gaseous sample volume of 1 L, the extrapolated limits of detections (LOD) were in the range 19.9–62.6 ng/m^3, depending on the PAH. Its analytical performances were then compared to those of the offline reference UHPLC-fluorescence method, widely used for airborne PAH monitoring. This was also compared with the very few portable or continuously operating instruments.

Keywords: polycyclic aromatic hydrocarbons (PAHs); continuous monitoring; GC-FID; UHPLC; fluorescence; automatic instrument; *in-situ* monitoring; airborne pollutants

check for updates

Citation: Vaz-Ramos, J.; Mascles, M.; Becker, A.; Bourgain, D.; Grandjean, A.; Bégin-Colin, S.; Amiet, F.; Bazin, D.; Le Calvé, S. Development of an Online Instrument for Continuous Gaseous PAH Quantification: Laboratory Evaluation and Comparison with The Offline Reference UHPLC-Fluorescence Method. *Chemosensors* **2023**, *11*, 496. https://doi.org/10.3390/chemosensors11090496

Academic Editor: Michele Penza

Received: 21 July 2023
Revised: 30 August 2023
Accepted: 6 September 2023
Published: 9 September 2023

Copyright: © 2023 by the authors. Licensee MDPI, Basel, Switzerland. This article is an open access article distributed under the terms and conditions of the Creative Commons Attribution (CC BY) license (https://creativecommons.org/licenses/by/4.0/).

1. Introduction

Polycyclic aromatic hydrocarbons (PAHs), a family of organic compounds with two or more fused aromatic rings in their structure, are widespread pollutants in major environmental media (water, air, and soil) [1,2]. Their production rates are known to have increased after the industrial revolution, and they persist ubiquitously in the environment [3]. Industrial processes, vehicle exhaust, domestic heating, and biomass combustion are among the main sources of PAH in the environment [4]. They are mostly introduced into the environment by their release into the atmosphere [5], but they can also easily enter soil and water bodies [6]. Therefore, humans can be exposed to them through different routes. PAHs are of great concern because they are toxic, mutagenic, and carcinogenic, and some of them are known endocrine disruptors, as is the case for benzo(a)pyrene (BaP) [3].

Thus, detecting and quantifying these pollutants in the environment is of the utmost importance. More than 100 PAHs are currently known, but the US Environmental Protection Agency (US EPA) has listed 16 compounds as priority PAHs [1]. Some European health agencies are now extending the number of PAHs monitored to include benzo(e)pyrene and benzo(j)fluoranthene [7]. Because of their associated health risks and persistent nature, they are heavily regulated. For example, the European Union established a mean annual target of 1 ng/m^3 for benzo(a)pyrene (BaP) in the air since BaP is considered the marker for PAH carcinogenicity [8].

In the air, PAHs are distributed between gaseous and particulate phases, with the latter corresponding to PAHs that are bound to airborne particulate matter. The low molecular weight (LMW) (2-ring and 3-ring) PAHs contribute dominantly to the gas phase, while the particulate phase is associated with HMW (5-ring and 6-ring) [9–11]. The MMW (4-ring) PAHs are often in both atmospheric phases, and their distribution will depend on the temperature and therefore on the season [9]. Their individual atmospheric concentrations are relatively low and typically in the range of pg/m^3 to ng/m^3 [12–14]. Even in the vicinity of industrial sites, individual concentrations of PAH remain in the ng/m^3 range [15].

When PAH emission from various industrial stacks (blast furnaces, basic oxygen furnaces, coke ovens, electric arc furnaces, heavy oil plants, power plants, and cement plants) was studied in southern Taiwan, Yang et al. reported ambient air individual PAH concentrations in the range 0.136–197 ng/m^3, depending on the PAH and sampling site, and a total PAH concentration between 198 and 298 ng/m^3 [16]. Consistently, the average total PAH concentration in the flue gas of 25 boiler stacks was around 490 µg/m^3 in the same country [17].

Chromatographic techniques are commonly used for the identification and quantification of PAH both in air samples and in other media such as water, soil, and food [6,14,18–21]. High-Performance Liquid Chromatography (HPLC) has been widely used for the analysis of PAHs, leading to highly selective and sensitive methods [3,14,22–24]. For the analysis of PAHs in air, HPLC is always used in offline mode since air samples must first be obtained on suitable filters and adsorbents to collect PAHs in the particulate and gas phases, respectively. The PAHs present in the air sample are then extracted, purified, and concentrated before analysis by HPLC coupled with fluorescence detection (FLD) [14,23–25]. The numerous sample processing steps are complicated procedures that can lead to significant errors in quantification. Gas chromatography (GC) methods coupled with detection using a mass spectrometer (MS) or alternatively other types of detectors are also frequently used and reported in the literature for the analysis of PAHs in the air [3,21,22,26]. All the GC-MS used are sedentary laboratory gas chromatographs, not able to work in online mode with continuous air sampling and analysis.

Given the low individual PAH concentrations in the air and their high toxicity at these low levels, highly efficient and sensitive analytical methods must be developed. As airborne PAH levels are generally low, it is necessary to integrate some preconcentration steps and/or develop some methods capable of detecting trace amounts of these compounds. Furthermore, most of the methods are offline techniques that can be time-consuming, expensive, and complicated and do not allow on-site monitoring of PAH [3]. If HPLC-FLD currently appears as the reference method, the ideal tool for PAH measurement is a portable (i.e., weight < 10 kg) or transportable (i.e., weight > 10 kg but easy to move, for example, with wheels), very sensitive, continuously operating, fully automatic, and remotely controlled instrument. Clearly, HPLC-FLD and GC-MS do not meet these specifications, especially if we add the cost aspect that must be considered if a wide deployment of a new analytical solution is expected. So far, to the best of our knowledge, only a few studies have reported on portable or transportable instruments for airborne PAH analysis, and they did not provide the possibility to perform online measurements because they were not equipped with an automatic sampling device enabling the collection of particulate and/or gaseous PAH. Conversely, some laboratory instruments have sampling facilities for either the gas or liquid phases [27,28], but they are not transportable. Despite the efforts of

scientists, it seems that there is no commercial portable/transportable device for continuous PAH quantification.

To tackle the drawbacks of the current analytical methods used for PAH quantification in air, the objective of this work was to develop a transportable instrument for continuous gas phase PAH analysis for at least the 16 PAHs regulated by the US EPA. The cost of the instrument and its robustness were also considered, which *de facto* ruled out the transportable GC-MS solution. The selected solution was a fully automatic GC-FID coupled to a preconcentration module already marketed by the company CHROMATOTEC, which was optimized in this work and evaluated under controlled laboratory conditions.

The analytical performances obtained were also compared to those of the offline reference method, i.e., UHPLC-FLD, usually used after sampling on adsorbent tubes (gas phase) or on filters (Particulate Matter (PM)), and further chemical extraction by accelerated solvent extraction (ASE), for example [14,23,24]. Both methods were evaluated in terms of sensitivity, repeatability, and linearity range and were compared with methods/instruments described in the literature that are either portable/transportable or automatic.

2. Materials and Methods

2.1. Development of Analytical Method by UHPLC-FLD/UV

A method for the detection and quantification of PAH was developed using Ultra High-Performance Liquid Chromatography coupled with fluorescence detection and UV detection (UHPLC-FLD/UV).

The UHPLC system consisted of a Nexera XR from Shimadzu and was equipped with a Knauer Ultrasep ES PAH-QC, 4 µm, 2 mm ID × 60 mm analytical column (Lot No.: 869/13) and its respective guard column. The system was equipped with a RF-20A XS fluorescence detector (Shimadzu) and a SPD-M30A UV detector (Shimadzu). The UHPLC method was developed based on recommendations given by KNAUER, and their analytical method was adapted and modified step by step to optimize the chromatographic separation [29]. The mobile phase was acetonitrile (ACN) and water with a flow rate of 0.5 mL/min and an elution gradient. The elution started with a ratio of 45:55 (ACN:Water) during the first 5 min; the amount of acetonitrile increased to 100:0 (ACN:Water) for 8 min; was stable for 6 min; before decreasing to 45:55 (ACN:Water) during 7 min. The initial conditions were reached at 26 min and were stable until the end of the run. The oven temperature was set to 30 °C. The sample was injected at 3 min to ensure the gradient had stabilized in the initial conditions, and the injection volume was fixed at 2 µL.

The compounds quantified in this analysis were the US EPA's 16 priority PAH: naphthalene (NAP), acenaphthylene (ACY), acenaphthene (ACE), fluorene (FLU), phenanthrene (PHE), anthracene (ANT), fluoranthene (FLE), pyrene (PYR), benzo(a)anthracene (BaA), chrysene (CHY), benzo(b)fluoranthene (BbF), benzo(k)fluoranthene (BkF), benzo(a)pyrene (BaP), dibenzo(a,h)anthracene (DahA), benzo(g,h,i)perylene (BghiP), indeno (1,2,3-cd)pyrene (IcdP). For the detection of PAH, the multi-channel mode of the fluorescence detector was used. PAH were detected at maximum excitation/emission wavelengths: 275/350 nm (NAP, ACE, FLU, PHE), 260/420 nm (ANT, PYR, BaA, CHY), 270/440 (FLE), 290/430 nm (BbF, BkF, BaP, DahA, BghiP), and 305/500 nm (IcdP). For the fluorescence acquisition, two different channels were used as follows: channel 1 first recorded excitation/emission wavelengths of 275/350 nm until t = 11.70 min, then switched to excitation/emission wavelengths of 270/440 nm, and finally to 290/430 nm at t = 18.00 min. For channel 2, it started with excitation/emission wavelengths of 260/420 nm and changed at 18.00 min to 305/500 nm. Since ACY is not detectable by fluorescence, it was detected and quantified with the UV detector at 229 nm, which corresponds to its absorbance maximum.

The PAH parent solution used was PAH Mixture 936 10–100 µg/mL in Acetonitrile (DRE-GA09000936AL) from Dr. Ehrenstorfer GmbH, with the following PAH concentrations (mg/L): NAP—101.7, ACY—100, ACE—100.4, FLU—101.6, PHE—99.89, ANT—99.6, FLE—9.95, PYR—10.17, BaA—9.93, CHY—9.907, BbF—10.01, BkF—4.97, BaP—9.94, DahA—9.94, BghiP—9.934, IcdP—10.01. This sample was further diluted in acetonitrile to obtain the

following daughter solutions for NAP: 0.515, 1.025, 4.91, 9.25, 20.11, 51.48, and 106.77 µg/L. For BkF, the corresponding concentrations were as follows: 0.025, 0.050, 0.24, 0.45, 0.98, 2.52, and 5.22 µg/L. This set of standard solutions was then used to establish the calibration curves for each PAH. Additionally, a blank with only acetonitrile was performed to account for interferences in the fluorescence/UV signal due to impurities present in acetonitrile. The limit of detection (LOD) and limit of quantification (LOQ) were determined based on the signal-to-noise approach. The LOD was considered to be the concentration for which the signal-to-noise ratio is 3. Similarly, a ratio of 10 was used for the LOQ.

Resolution (R), which indicates the separation between two peaks, was determined using the tangent method. The repeatability and reproducibility of the analytical method were assessed, and the respective RSD (relative standard deviation) was determined. For repeatability, the same standard sample was analyzed four times on the same day, while for reproducibility, the same standard sample was analyzed on three different days. The concentrations of the PAH standard used for the evaluation of repeatability and reproducibility were in the range 0.98–20.11 µg/L, i.e., 20.11 µg/L for NAP and 0.98 µg/L for BkF.

2.2. Development of Analytical Method by GC-FID

Based on a commercially available gas chromatograph (GC) equipped with flame ionization detection (FID) used for the analysis of volatile organic compounds (VOC) with C6-C12 and equipped with a preconcentrator (Airmo C6–C12), a new GC-FID dedicated to the analysis of PAHs was developed in this work. Initially, the same components of the instrument were retained, including the preconcentrator, but they were adapted to withstand higher temperatures. While adsorption at the preconcentrator was effective, desorption of the 4–6 rings of PAH remained ineffective. This is why, in a second phase, a new two-stage preconcentration module was specially designed to finally obtain the instrument airmo C6-C20+ (CHROMATOTEC, Saint-Antoine, France). The schematic of this GC-FID is shown in Figure 1, with the instrument being equipped with a syringe injector for calibration purposes. This is a transportable model (222 mm × 482 mm × 600 mm; 22 kg) that allows *in-situ* measuring and remote monitoring (Figure S1).

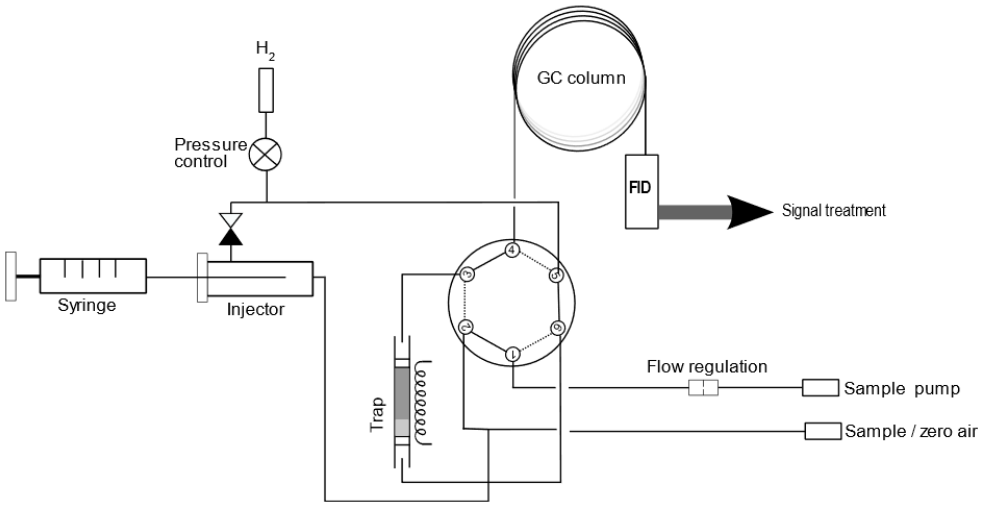

Figure 1. Simplified schematic diagram of the instrument airmoVOC C6-C20+ equipped with an FID detector and a syringe injector.

A method for the analysis of PAH in the air was then developed using the instrument airmo C6–C20+ (CHROMATOTEC, France). A stock solution containing 18 PAH, i.e., the same 16 PAH as above plus 1-methyl naphthalene (1Me-NAP) and 2-methyl naphthalene (2Me-NAP), at 2000 µg/mL each in dichloromethane (Restek), was used to prepare different daughter solutions in dichloromethane at the following concentrations: 9.91, 5.34, and

2.14 µg/mL. This last solution of PAH at 2.14 µg/mL was then diluted approximately 10 times in dichloromethane to obtain a 0.23 µg/mL solution. This latter concentration was chosen because it was slightly higher than the quantification limit (see Section 3.2), enabling it to display all the peaks on the chromatogram.

For the GC-FID analysis, the timeline of events is shown in Figure S2. The total duration of a cycle is about 1 h, but it is split into different subparts, i.e., the synchronization of the different GC elements (1 min), the vaporization of PAH from a liquid solution manually injected into the GC injector simultaneously with sampling on the preconcentrator adsorbents (5 min), the desorption step (8 min), and the chromatogram acquisition (45 min).

First, 1 µL of a PAH solution diluted in dichloromethane was manually injected using a precise liquid syringe (sge TRAJAN 1BR-7—1 µL) into the injector regulated at 250 °C to vaporize the entire mixture, which is swept by a flow of hydrogen at a rate of 7 mL/min for 300 s, thus mimicking a gaseous sample of a PAH mixture. The resulting injected masses of each PAH were as follows: 9.91 ng, 5.34 ng, 2.14 ng, and 0.23 ng. This gas mixture was then passed through a two-stage preconcentration device kept at room temperature. The first stage of the preconcentration unit is made of stainless-steel tubing and is used to cool down the sample and induce adsorption of non-volatile PAH (more than 3 aromatic rings). The second stage is a glass tube filled with a mixture of Carbotrap B and C adsorbents to perform preconcentration and thermodesorption of semi-volatile PAH (2 and 3 aromatic rings). The composition and geometry of the preconcentration device will not be detailed here for reasons of confidentiality. No split was used for the transfer of analytes from the injector to the preconcentrator. The entire PAH content injected into the liquid injector was thus theoretically transferred to the adsorbent-filled trap.

Once the adsorption stage was complete, the two stages of the preconcentration unit were then rapidly heated to 350 °C in about 60 s. This temperature was maintained for 480 s during the desorption phase of the analytes and flushed with hydrogen carrier gas at a flow rate of 9 mL/min. Again, no split was used for the transfer from the preconcentrator to the column. The PAH were then separated using a 30 m long MXT-1 GC column with an internal diameter of 0.53 mm and a film thickness of 0.25 µm before arriving one by one at the FID detector. The temperature gradient of the oven was optimized and set as follows: from 38 to 50 °C at a rate of 2 °C/min (360 s), from 50 to 80 °C at a rate of 10 °C/min for 180 s, from 80 to 220 °C at a rate of 15 °C/min (560 s), from 220 to 320 °C at a rate of 10 °C/min (600 s), and finally 320 °C for 1000 s. For detection, the FID temperature was set at 350 °C, and the FID detector was supplied with 350 mL/min of zero air and 50 mL/min of hydrogen, both gases being provided by two generators (airmoPure and Hydroxychrom from Chromatotec for zero air and hydrogen, respectively). Once the chromatogram acquisition was complete, the peaks were automatically integrated, and the data were saved for further data treatment.

The repeatability of the GC-FID analytical method was evaluated, and the corresponding RSD (relative standard deviation) was determined. For this, the same standard PAH mixture solution was manually injected and analyzed three times on the same day. Peak resolution (R) was again determined using the tangent method.

2.3. Determination of the Chromatographic Resolution

The chromatographic resolution (R) between two consecutive peaks was calculated according to the tangent method with Equation (1):

$$R = \frac{t_{R1} - t_{R2}}{\frac{1}{2}(W_1 + W_2)} \quad (1)$$

where t_{R1} and t_{R2} are the retention times (min) of two consecutive peaks; and W_1 and W_2 are the tangent widths of the two consecutive peaks at the baseline.

The software of both instruments provided the values for retention time for each peak, whereas the tangent widths were either provided by UHPLC software or calculated

using Excel for the GC-FID. For each compound, the resolution was defined as the lowest resolution value between the resolution with its preceding peak and the resolution with its following peak.

3. Results

The reference method currently used is HPLC or UHPLC coupled with fluorescence detection for the analysis of the 16 USEPA PAHs. For the GC method, EPA method 8310 is commonly used, which incorporates the same 16 PAHs plus two methyl naphthalene compounds to test for interferences linked to the presence of these compounds. In addition, it was interesting to add some LMW PAH with high partitioning in air because the GC-FID technique is devoted to directly analyzing the compounds in the gas phase.

3.1. Development of Analytical Method by UHPLC-FLD/UV

In Figure 2, the typically obtained chromatograms with the UHPLC-FLD/UV method are presented for the PAH detected by fluorescence. The fluorescence detector allows the use of up to four channels operating in parallel with different couples of excitation/emission wavelengths. In the developed method, only two channels were used, which made it possible to ensure that the change of excitation/emission wavelengths did not occur in the middle of a peak. This was particularly important for the last three peaks (DahA, BghiP, and IcdP), which had very close retention times but two different excitation/emission wavelengths. The method was optimized to ensure good separation, as displayed in Figure 2 for the 15 peaks detected by fluorescence, where there was only slight co-elution of the peaks of BaA and CHY and of BkF and BaP, and partial co-elution of DahA and BghiP. ACY is not fluorescent and was easily detected by UV at 229 nm (Figure S3).

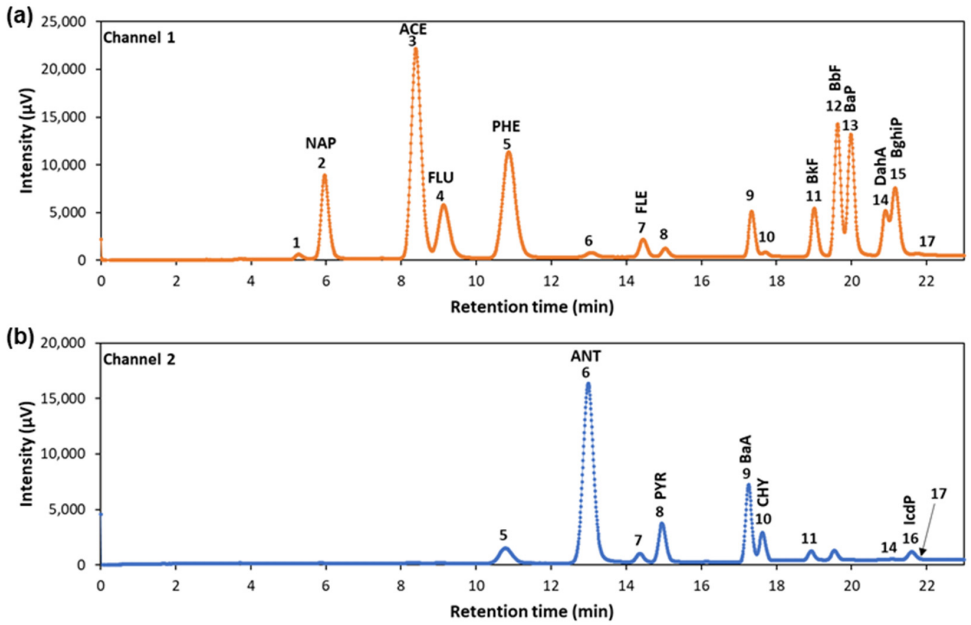

Figure 2. Chromatograms of the developed UHPLC-FLD/UV method for the two used FLD channels, obtained with an injection volume of 2 µL and a PAH concentration of 2.52 (BkF) to 51.48 (NAP) µg/L depending on the PAH. The chromatograms were obtained with (**a**) channels 1 and (**b**) 2. Each chromatographic peak is labeled with a peak number: 1, injection peak; 2, NAP; 3, ACE; 4, FLU; 5, PHE; 6, ANT; 7, FLE; 8, PYR; 9, BaA; 10, CHY; 11, BbF; 12, BkF; 13, BaP; 14, DahA; 15, BghiP; 16, IcdP; 17, impurity of ACN. Channel 1 recorded excitation/emission wavelengths of 275/350 nm until t = 11.70 min, then switched to excitation/emission wavelengths of 270/440 nm, and finally switched at t = 18.00 min to 290/430 nm. Channel 2 started with excitation/emission wavelengths of 260/420 nm and changed at 18.00 min to 305/500 nm.

In Figure 2, PAH species are visible on the chromatogram used to quantify them. However, they may also be visible on the other chromatograms despite the non-optimal excitation/emission wavelengths used for the fluorescence detection. In channel 1, peaks 6, 8, and 10 correspond to ANT, PYR, and CHY, respectively. In channel 2, peaks 5, 7, 11, and 14 correspond to PHE, FLE, BbF, and DahA. Peak 17, displayed at the end of the chromatogram in channel 1 and 2, correspond to an impurity of Acetonitrile. In channels 1, peak 1 corresponds to the injection peak, which is almost unseen in channel 2. In Figure 2, the peaks used for quantification bear the labels of the compounds, i.e., from NAP to BghiP and from ANT to IcdP for channels 1 and 2, respectively.

To assess the PAH separation provided by UHPLC-FLD/UV, peak resolutions R were also determined using the tangent method. The values of R, which are gathered in Table 1, were usually higher than 1.5, indicating a good separation for PAH species. However, the last three PAH (DahA, BghiP, and IcdP) had the lowest resolution with values of R(DahA—BghiP) = 0.50 (channel 1) and R(IcdP—Peak 17) = 0.77 (channel 2), where peak 17 corresponded to an unidentified impurity of ACN.

Table 1. Peak resolutions for all PAH obtained with the developed UHPLC-FLD/UV method. The labels of chromatographic peaks are detailed in the text and the caption of Figure 2.

Channel 1 for Fluorescence	R [a]	Channel 2 for Fluorescence	R [a]
Peak 1 (5.27 min)–NAP (5.96 min)	1.87	Peak 5 (10.80 min)–ANT (12.99 min)	3.77
NAP (5.96 min)–ACE (8.39 min)	5.44	ANT (12.99 min)–Peak 7 (14.34 min)	3.02
ACE (8.39 min)–FLU (9.13 min)	1.31	Peak 7 (14.34 min)–PYR (14.95 min)	1.55
FLU (9.13 min)–PHE (10.86 min)	2.74	PYR (14.95 min)–BaA (17.26 min)	6.78
PHE (10.86 min)–Peak 6 (13.07 min)	3.76	BaA (17.26 min)–CHY (17.63 min)	1.15
Peak 6 (13.07 min) –FLE (14.45 min)	3.16	CHY (17.63 min)–Peak 11 (18.93 min)	4.04
FLE (14.45 min)–Peak 8 (15.04 min)	1.56	Peak 14 (21.11 min)–IcdP (21.61 min)	5.64
Peak 10 (17.71 min)–BbF (19.01 min)	3.63	IcdP (21.61 min)–Peak 17 (22.04)	0.77
BbF (19.01 min)–BkF (19.62 min)	1.91		
BkF (19.62 min)–BaP (19.99 min)	1.08	**UV detection**	R
BaP (19.99 min)–DahA (20.91 min)	2.05	Peak 18 (5.88 min)–ACY (6.69 min)	2.33
DahA (20.91 min)–BghiP (21.16 min)	0.50		
BghiP (21.16 min)–Peak 17 (21.75 min)	1.33		

[a] Background color: green for peak resolution R > 1.5; yellow for 1 < R < 1.5; red for R < 1.

Calibration curves were obtained for the 16 PAH with the UHPLC-FLD/UV method. Figure 3 shows three representative examples of PAH calibration curves, namely for NAP, PYR, and BaP. In addition, the individual curve for each PAH can be found in Figure S4. The obtained linear equations and R^2, as well as the range of concentration where the calibration curve is valid, are listed in Table 2. LOD and LOQ values, as well as RSD values for repeatability and reproducibility, can also be found in Table 2.

As shown in Table 2, the calibration curves were linear for the studied ranges, with very good R^2 values (>0.998). All the calibration curves were obtained with the y-intercept = 0, except for IcdP. In fact, for this species, a residual peak was observed in the ACN blank at the same retention time and excitation/emission wavelengths as IcdP. This result was considered for the calibration curve, which explains the non-zero y-intercept = 1113.9 (see Table 2).

LOD and LOQ values of the UHPLC method were obtained for all the PAH (see Table 2). ACY showed the worst sensitivity, which is not unexpected considering that this compound was detected by UV and not by fluorescence. For the PAH detected by fluorescence, the LOD varied between 0.005 and 0.530 µg/L, and BkF, BaP, and IcdP exhibited the best sensitivity.

Table 2. Calibration curve equations, LOD and LOQ values (in µg/L, pg, and pg/m^3), repeatability, and reproducibility results of the developed UHPLC-FLD/UV method.

PAH	Calibration Curve			LOD (µg/L)	LOQ (µg/L)	LOD^{mass} (pg) [a]	LOQ^{mass} (pg) [a]	LOD^{air} (pg/m^3) [b]	LOQ^{air} (pg/m^3) [b]	Repeat-Ability (RSD,%) [c]	Reproducibility (RSD,%) [c]
	Equation	R^2	Range (µg/L)								
NAP	y = 2395.9x	0.9992	0.52–107	0.174	0.580	0.348	1.160	1.16	3.87	1.37	1.77
ACY	y = 56.592x	0.9969	0.51–105	1.322	4.407	2.644	8.815	8.81	29.38	1.82	2.54
ACE	y = 8180.1x	0.9993	0.51–105	0.292	0.972	0.583	1.943	1.94	6.48	0.04	2.22
FLU	y = 2306.6x	0.9996	0.52–107	0.530	1.766	1.059	3.531	3.53	11.77	0.98	6.03
PHE	y = 5387.5x	0.9995	0.51–105	0.152	0.506	0.304	1.012	1.01	3.37	0.54	1.41
ANT	y = 6010.9x	0.9999	0.51–105	0.136	0.455	0.273	0.909	0.91	3.03	0.57	3.25
FLE	y = 5379.8x	0.9982	0.05–10	0.018	0.060	0.036	0.120	0.12	0.40	1.51	9.01
PYR	y = 9454.9x	0.9998	0.05–11	0.058	0.193	0.116	0.385	0.39	1.28	0.74	0.65
BaA	y = 15785x	0.9993	0.05–10	0.090	0.300	0.180	0.600	0.60	2.00	1.01	0.58
CHY	y = 6203.6x	0.9994	0.05–10	0.037	0.124	0.074	0.248	0.25	0.83	6.74	1.78
BbF	y = 11839x	0.9994	0.05–11	0.023	0.077	0.046	0.154	0.15	0.51	0.74	0.74
BkF	y = 66157x	0.9992	0.025–5	0.005	0.015	0.009	0.031	0.03	0.10	0.81	1.06
BaP	y = 19785x	0.9998	0.05–10	0.013	0.043	0.026	0.086	0.09	0.29	2.16	6.17
DahA	y = 11429x	0.9982	0.05–10	0.024	0.080	0.048	0.160	0.16	0.53	3.33	1.32
BghiP	y = 17895x	0.9997	0.05–10	0.020	0.068	0.041	0.136	0.14	0.45	3.09	12.21
IcdP	y = 2010.3x + 1113.9	0.9996	0.05–11	0.008	0.028	0.017	0.056	0.06	0.19	0.37	20.83

[a] LOD^{mass} and LOQ^{mass} are the conversion of the LOD and LOQ obtained in µg/L into mass by multiplying by the injection volume of 2 µL. [b] LOD^{air} and LOQ^{air} are the conversion of the LOD and LOQ (in µg/L) into an air PAH concentration by dividing by a final extract volume (offline preconcentration step) of 1 mL and multiplying by a sampling volume of air of 150 m^3, according to a previous study [24]. [c] Repeatability and reproducibility were studied with a PAH mixture concentration of 0.98–20.11 µg/L, depending on the PAH.

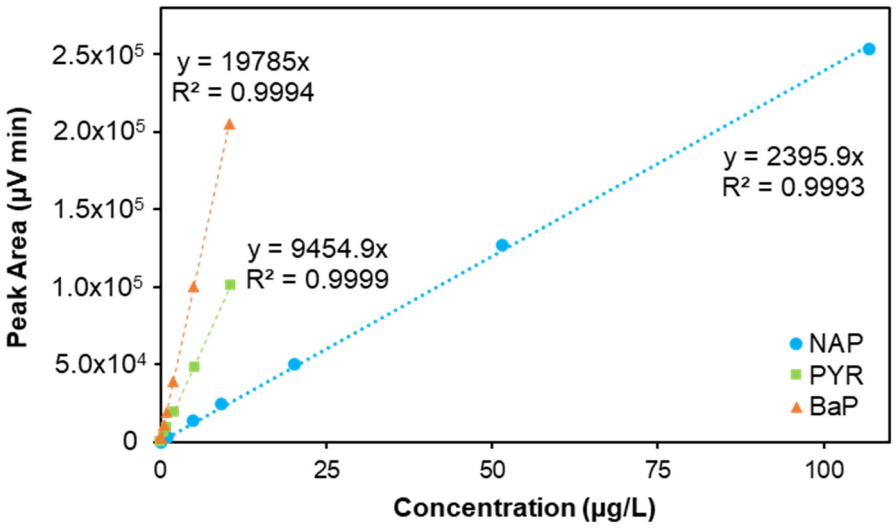

Figure 3. Chromatographic peak area versus PAH concentration (in µg/L) obtained by UHPLC-FLD/UV. The dashed line corresponds to the linear regression in the investigated concentration ranges of 0.52–107 µg/L for NAP, 0.05–11 µg/L for PYR, and 0.05–10 µg/L for BaP, with an injection volume of 2 µL.

Repeatability and reproducibility results are also summarized in Table 2. Good repeatability was generally observed with RSD lower than 3.3%, except for CHY, where RSD reached 6.7%. For CHY, this may be explained by the uncomplete separation with BaA (R = 1.15) as illustrated in Figure 2b, leading to a higher uncertainty in peak area determination. Regarding reproducibility, higher RSD values were obtained, with values usually lower than 6.2% except for FLE, IcdP and BghiP. These two PAHs had the longest retention time. These two 6-ring PAH showed therefore the worst reproducibility, with RSDs that reached 20.8 and 12.2%, respectively, which might be related to their poor resolution and the presence of an impurity in ACN. For FLE, the low intensity of the peak (Figure 2a) could explain the relatively poor reproducibility with a high RSD of 9.0%.

3.2. Development of Analytical Method by GC-FID

Figure 4 shows a typical chromatogram obtained by GC-FID for the mixture of the 18 PAH. Unexpectedly, the three last peaks are less intense compared to the others. Typically, the FID detector response factor is proportional to the number of carbon atoms in the molecule. But here, the lowering trend in response factors may suggest that the heaviest PAHs are partially lost inside the GC-FID instrument. Using the separation method optimized in this work, 10 of the 18 PAHs are perfectly separated (see Figure 4) with a chromatographic resolution higher than 1.5 (see Table 3). The retention times of the 18 PAH are reported in Tables 3 and 4. Figure 4 shows that eight species are still partially co-eluted two by two. The two isomers, namely Benzo(k)fluoranthene (t_R = 1609.5 s) and benzo(b)fluoranthene (t_R = 1609.5 s), are fully co-eluted and exhibit the same retention time, leading obviously to a chromatographic resolution of R = 0.00 (see Table 3). Benzo(a)anthracene (t_R = 1460.0 s) and chrysene (t_R = 1462.8 s) are then the most co-eluted with an R value of 0.23. Phenanthrene (t_R = 1131.4 s) and anthracene (t_R = 1136.9 s) are also partially co-eluted (R = 1.07). The two last co-eluted species are Indeno(1,2,3-cd)pyrene (t_R = 1786.7 s) and dibenzo(a,h)anthracene (t_R = 1795.1 s), which exhibited an insufficient separation characterized by a chromatographic resolution of R = 1.30.

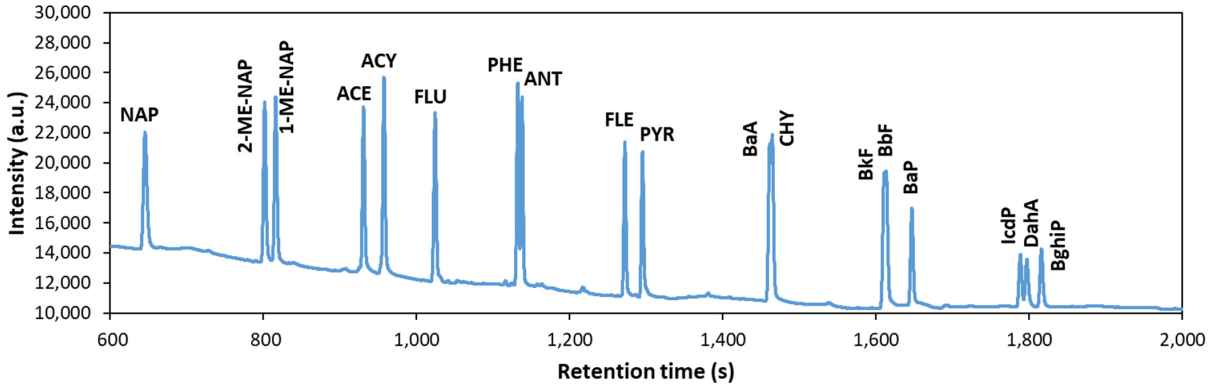

Figure 4. Chromatogram obtained with the GC-FID method using the developed AirmoVOC C6-C20+ instrument and with the injection of 1 µL of a solution of 18 PAH, each with a concentration of 9.9 µg/mL, i.e., 9.91 ng of each PAH.

Table 3. Peak resolutions for all 18 PAH obtained with the GC-FID method using the developed AirmoVOC C6-C20+ instrument.

Peaks	R [a]
NAP (646.4 s)–2Me-NAP (801.7 s)	21.28
2Me-NAP (801.7 s)–1Me-NAP (816.0 s)	2.32
1Me-NAP (816.0 s)–ACE (930.5 s)	19.34
ACE (930.5 s)–ACY (957.1 s)	4.62
ACY (957.1 s)–FLU (1023.6 s)	11.18
FLU (1023.6 s)–PHE (1131.4 s)	19.09
PHE (1131.4 s)–ANT (1136.9 s)	1.07
ANT (1136.9 s)–FLE (1271.1 s)	26.04
FLE (1271.1 s)–PYR (1294.1 s)	4.36
PYR (1294.1 s)–BaA (1460.0 s)	18.55
BaA (1460.0 s)–CHY (1462.8 s)	0.23
CHY (1462.8 s)–(BbF + BkF) (1609.5 s)	14.01
BkF (1609.5 s)–BbF (1609.5 s)	0.00
(BbF + BkF) (1609.5 s)–BaP (1645.2 s)	4.58
BaP (1645.2 s)–IcdP (1786.7 s)	21.90
IcdP (1786.7 s)–DahA (1795.1 s)	1.30
DahA (1795.1 s)–BghiP 1814.0 s)	2.84

[a] Background color: green for peak resolution R > 1.5; yellow for 1 < R < 1.5; red for R < 1.

Table 4. Calibration curves, LOD and LOQ values, and repeatability results of the GC-FID method using the developed AirmoVOC C6-C20+ instrument.

PAH	t_R (s)	Calibration Curve			LOD^{mass} (pg)	LOQ^{mass} (pg)	LOD^{air} (ng/m^3) [a]	LOQ^{air} (ng/m^3) [a]	Repeat-Ability [b] (RSD,%)
		Equation	R^2	Range (ng)					
NAP	646.4	y = 4321.1x −16.919	0.9997	0.230–9.91	39.0	130.0	39.0	130.0	3.54
2Me-NAP	801.7	y = 4136.3x +431.1	0.9996	0.230–9.91	27.2	90.5	27.2	90.5	3.70
1Me-NAP	816.0	y = 4212.8x + 414.45	0.9995	0.230–9.91	26.0	86.4	26.0	86.4	3.72
ACE	930.5	y = 4147x + 428.12	0.9994	0.230–9.91	27.2	90.5	27.2	90.5	2.66
ACY	957.1	y = 4731.4x + 977.82	0.9989	0.230–9.91	22.3	74.3	22.3	74.3	6.20
FLU	1023.6	y = 4365.5x + 549.82	0.9989	0.230–9.91	24.3	81.0	24.3	81.0	4.28
PHE	1131.4	y = 4138.3x + 685.85	0.9992	0.230–9.91	19.9	66.3	19.9	66.3	2.45
ANT	1136.9	y = 4076.6x − 133.46	0.9993	0.230–9.91	25.0	83.4	25.0	83.4	1.34
FLE	1271.1	y = 3334.3x + 180.83	0.9988	0.230–9.91	26.9	89.7	26.9	89.7	3.57
PYR	1294.1	y = 3428.1x + 333	0.9990	0.230–9.91	28.0	93.4	28.0	93.4	2.28
BaA	1460.0	y = 3813.3x + 1015.1	0.9987	0.460–19.82	42.7 [c]	142.3 [c]	42.7 [c]	142.3 [c]	5.30
CHY [c]	1462.8								
BbF + BkF [c]	1609.5	y = 3158x + 2081.9	0.9947	0.460–19.82	40.1 [c]	133.4 [c]	40.1 [c]	133.4 [c]	5.29
BaP	1645.2	y = 2463.9x + 791.54	0.9907	0.230–9.91	29.0	96.4	29.0	96.4	5.56
IcdP	1786.7	y = 1436.4x + 532.49	0.9848	0.230–9.91	48.0	159.8	48.0	159.8	9.84
DahA	1795.1	y = 1477.1x + 317.19	0.9933	0.230–9.91	62.6	208.5	62.6	208.5	8.94
BghiP	1814.0	y = 1719x + 853.67	0.9824	0.230–9.91	42.7	142.3	42.7	142.3	15.44

[a] LOD^{air} and LOQ^{air} are the conversion of the LOD and LOQ (in pg) into an airborne PAH concentration, considering a sampling volume of air of 1 L (1×10^{-3} m^3). [b] The repeatability was studied for injected masses of each PAH equal to 5.34 ng by repeating the analysis on the same day. [c] For compounds co-eluted and quantified together, the LOD calculation was performed taking into account the total concentration of the two compounds.

By varying the injected mass between 0 and 9.91 ng, a linear calibration curve was plotted for each PAH, as shown in Figure 5 for three representative PAH, namely NAP, PYR, and BaP, and for all 18 studied PAH (see Figure S5). The details of the linearity results obtained with the GC-FID method for each PAH are summarized in Table 4. Because of their non-existent or insufficient separations, the pairs BkF + BbF and BaA + CHY were quantified together. The slope of the linear regression decreased for the heaviest PAH, which supports the idea of a partial loss of heavy PAH in the instrument. The linear regression coefficient R^2 was higher than 0.99 in most cases, except for indeno(1,2,3-cd)pyrene (IcdP) and benzo(g,h,i)perylene (BghiP), with R^2 values of 0.984 and 0.982, respectively. Despite their potential loss inside the GC-FID, the heaviest PAH (DahA, BghiP, and IcdP) exhibited excellent linearities.

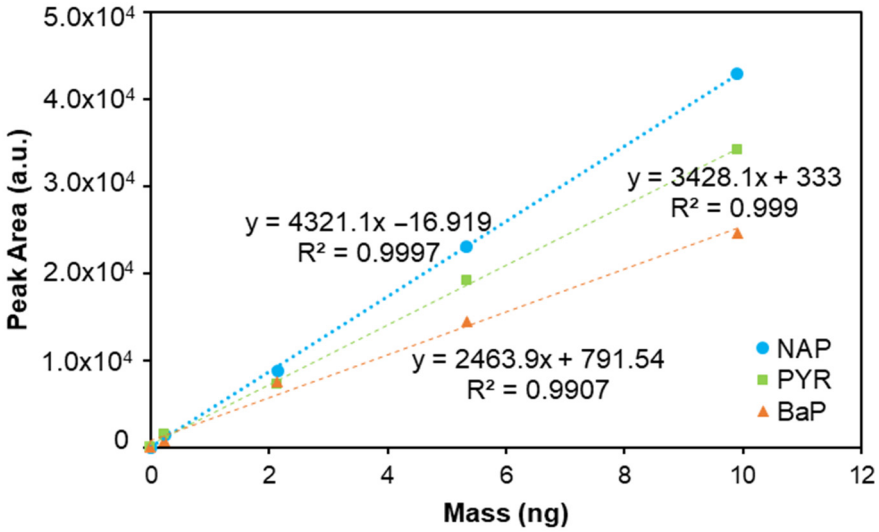

Figure 5. Chromatographic peak area versus PAH mass injected at the GC injector of the AirmoVOC C6-C20+ instrument (GC-FID method), allowing vaporization of PAH to mimic gas phase concentrations. The dashed line corresponds to the linear regression in the investigated concentration range, i.e., between 0 and 9.91 ng for NAP, PYR, and BaP. These PAH masses were obtained by injecting 1 µg/L of a standard PAH mixture solution of 0–9.9 µg/mL.

The detection and quantification limits were again determined based on the signal-to-noise approach by considering the signal-to-noise ratios of 3 and 10, respectively. Table 4 reports the LOD, the LOQ, and the repeatability determined in our experimental conditions for every PAH using the AirmoVOC C6-C20+ instrument (GC-FID method) developed in this work. The resulting LOD is in the range of 19.9–62.6 pg, depending on the PAH. Repeatability was evaluated from the analysis of injected masses of each PAH equal to 5.34 ng by repeating the analysis on the same day. Reproducibility was not fully evaluated, but the linear plot in Figure 5 was obtained from GC analysis performed on different days, suggesting good reproducibility as well.

4. Discussion

The results are discussed here in terms of chromatographic resolution and sensitivities. The performance of the two methods developed in this work is compared with each other and with instruments operating continuously and in real time.

4.1. Chromatographic Resolution of Both Instruments

The chromatographic resolution is plotted against the separated molecules as a bar graph (see Figure 6). Chromatographic resolution is considered good for R > 1.5 (green color), relatively satisfactory for 1.5 < R < 1 (orange color), and insufficient for R < 1 (red color). As illustrated in Figure 6, neither developed method provides a perfect resolution of all peaks. In terms of resolution, the two methods are comparable. Neither method allows the complete separation of the PAH analysis. However, higher peak resolution values were generally obtained with the GC-FID method, a consequence of the much thinner peaks obtained with this method (see Figures 2 and 4).

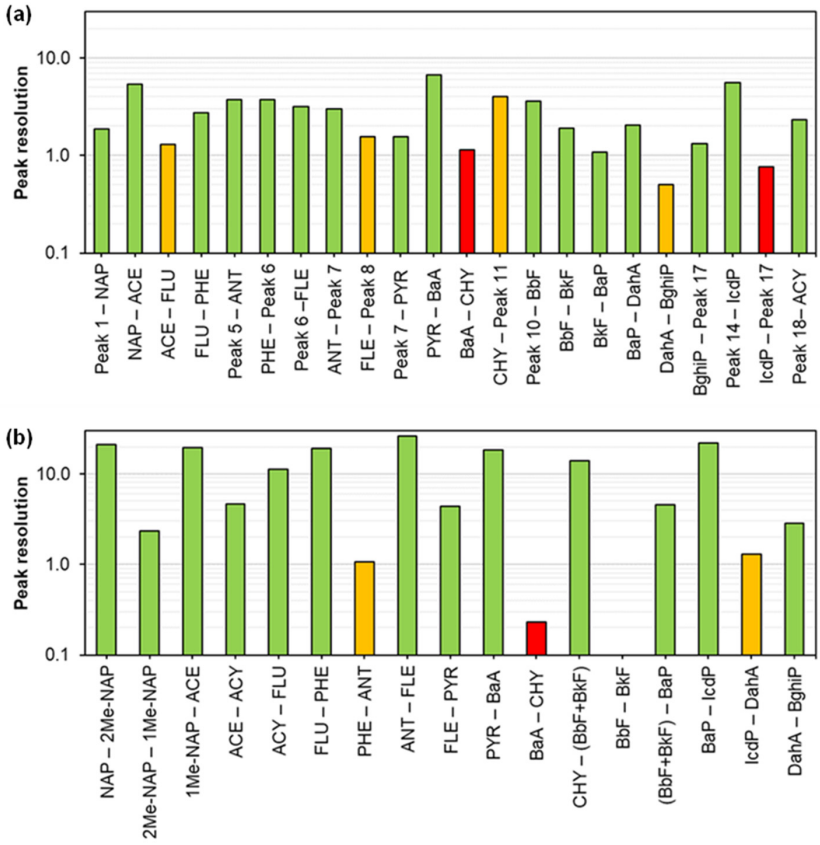

Figure 6. Peak resolution obtained for (**a**) the 16 US EPA PAH determined by the UHPLC-FLD/UV method and (**b**) the 18 PAH determined by the GD-FID method. The PAHs are presented in order of elution. Background color: green for peak resolution R > 1.5; yellow for 1 < R < 1.5; red for R < 1.

4.2. Sensitivity of Both Instruments

Given the individual concentrations of PAH in the gas phase in the atmosphere, which generally vary between 0.1 and 1 ng/m^3 [12,13,23,24], a quantification limit of the order of 0.1 ng/m^3 could be ideally targeted for an online analysis system.

The injected mass quantification limits obtained are compared in Figure 7 for both instruments, i.e., UHPLC-FLD/UV and GC-FID. In GC-FID, the quantification limit is of the order of one hundred pg, whereas in UHPLC-FLD, the quantification limit ranges roughly between 0.03 and 3.5 pg. For ACY, which is detected by UHPLC-UV, the LOQ is equal to about 8.8 pg in UHPLC-UV.

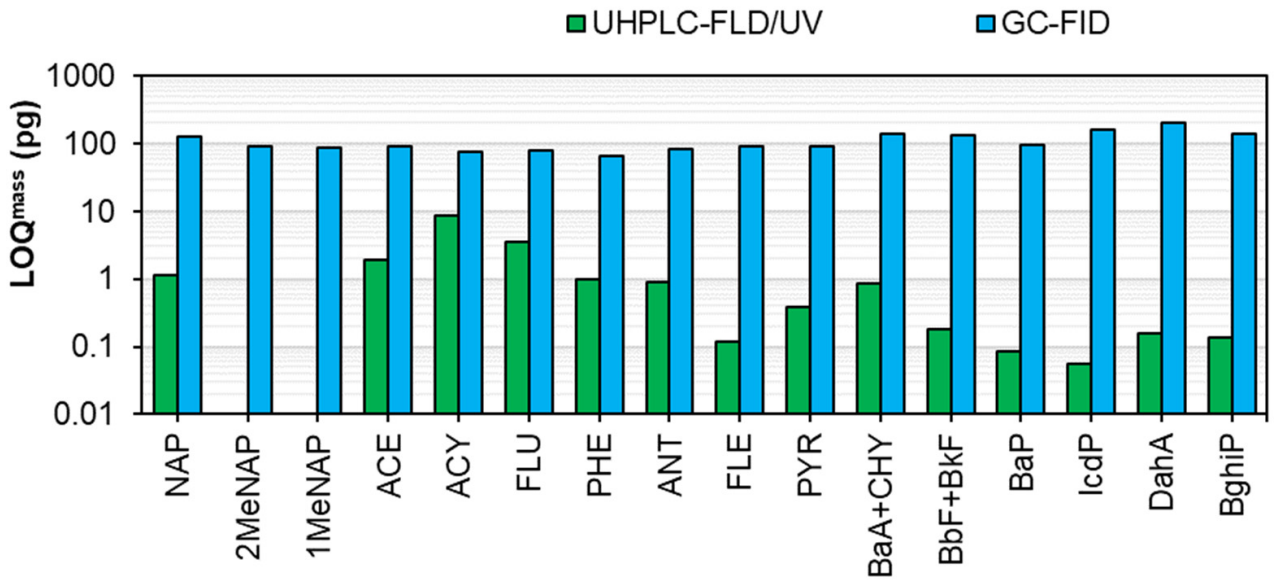

Figure 7. Limits of quantification in mass for the 16 US EPA PAH determined by the UHPLC-FLD/UV method and the 18 PAHs determined by the GD-FID method. In comparison to the GC method, in the UHPLC method, the sum of the LODs of BaA and CHY and of BbF and BkF is represented. The PAH are presented in order of elution by the GC method.

Intrinsically, UHPLC is therefore more sensitive. Nevertheless, it does not allow for online and continuous analysis of PAH in the air with a fully automatic instrument. UHPLC-FLD generally allows for offline analysis after trapping the gaseous PAH on an adsorbent and chemical desorption with a suitable solvent before injection of the eluted solution through the UHPLC injection loop. Although this technology could be automated with automatic elution of the adsorbent tubes, continuous analysis remains problematic as the adsorbent would have to be dried between two analyses for reconditioning before the next air sampling. In addition, this would require a large supply of potentially toxic solvent to allow operation over long periods, even if the quantity of elution solvent is limited to 5 mL per analysis. In contrast to offline methods using UHPLC-FLD, a sample preconcentration step via a fully automated system remains extremely complex.

A quantification limit of 0.3 pg typically obtained in this work by UHPLC-FLD with an injected volume of 2 µL (see Table 2) corresponds to an individual PAH amount of 750 pg in 5 mL of a solution resulting from the adsorbent elution. Based on a sampling volume of 1 L (1×10^{-3} m^3) and a flow rate of 40 mL/min, a sampling time of 25 min is needed. If no additional sample preconcentration step is considered between the adsorbent elution and UHPLC analysis, the resulting LOQ of individual PAH in the air will then be 750 ng/m^3 (750 pg/1×10^{-3} m^3). This simple calculation tends to show that the UHPLC-FLD method, with no preconcentration step, does not achieve the target value of the quantification limit of 0.1 ng/m^3.

In contrast, continuous analysis with the GC-FID instrument developed in this work seems easily accessible. With a sample of 1 L of air, for example, at a flow rate of 20 mL/min for 50 min, it is possible to quantify concentrations of PAH by GC-FID varying between 66.3 and 208.5 ng/m^3 in the gas phase (see Table 4), depending on the PAH.

With 24 h sampling at a flow rate of 50 mL/min, which corresponds to a single sampled air volume of 72 L per day, the LOQs for GC-FID and UHPLC-FLD are then equal to 0.92–2.90 ng/m^3 and 10.4 ng/m^3, respectively. For GC-FID, these quantification limits come close to the target sensitivity, but this would imply only one sample per day, which corresponds to a time resolution that may be insufficient depending on the case and the needs.

In light of the above arguments, despite a lower intrinsic sensitivity (expressed in pg injected), GC-FID appears more promising and suitable for online PAH analysis. Indeed, in continuous mode with a sample volume restricted to 1 L, the sensitivity of UHPLC-FLD is about 4–12.6 times lower than that of GC-FID, depending on the PAH considered.

4.3. Comparison with the Literature

Some analytical techniques allow real-time measurements of the total amount of PAH in different matrices. For particle-bound polycyclic aromatic hydrocarbons (PPAH), the photoelectric aerosol sensor (PAS) is a technique suitable for their online monitoring [30]. For water samples, commercial sensors based on fluorimetry can measure total PAH concentrations, typically from 0 to 1000 µg/L [31].

When PAH speciation is considered, many studies were carried out on the measurement of PAH in the air [13,23,24,26,32–34] or water [35,36], but the vast majority used offline and non-automatic methods.

Some studies were already carried out with offline GC-FID PAH measurements for the analysis of water combined with SPME, SPE, or MSPE [35–37], soil samples after solid-liquid extraction [38], or food samples after SPE extraction [39,40]. However, none have integrated an automatic and programmable sampling and extraction module, or portable instruments for *in-situ* measurements. Whatever, it is interesting to note that Carvalho et al. report a chromatogram in their Figure 3 [36] that is very similar to that in our Figure 4, which tends to confirm that some of the heaviest PAH (DahA, BghiP, and IcdP), which have the longest retention times, are probably partially lost in the instrument as already suggested in Section 3.2.

In the following part of this section dedicated to the comparison with the literature, it was decided to restrict the comparison to methods that had at least one of the two priority characteristics sought, namely portability/transportability or a fully automatic aspect for both sampling and analysis. Only a few studies report either automatic or portable instruments for the measurement of individual PAH in the liquid or gas phase [27,28,41,42] (see Table 5). In opposition to Section 4.2., LOD was reported instead of LOQ in Table 5 since this value is reported by default in the literature.

About the portable/transportable instrument, Chatzimichail et al. reported the development of a handheld HPLC equipped with an absorption detector capable of identifying 24 PAH (including the 16 US EPA ones) based on their characteristic spectral absorption profiles [41]. This portable HPLC is compact, with the following dimensions: 25.5 cm wide, 25.0 cm deep, and 12.6 cm high. This miniaturized device allows for very good sensitivity for all the PAH, as illustrated by the BaP LOD value of 0.014 ng/L without any sample preconcentration. However, the manual injection of the sample did not allow for continuous measurement. In general, gas chromatography coupled with mass spectrometry (GC-MS) allows for the identification and quantification of volatile and semi-volatile organic compounds at low concentration levels [43]. The applicability of portable field GC-MS for the rapid sampling and measurement of high-boiling semi-volatile organic compounds, including PAH, was investigated in environmental samples [42] by using a Torion T-9 portable GC-MS (PerkinElmer) equipped with a toroidal ion trap mass spectrometer covering a mass range from 43 to 500 Daltons [44]. Although this portable GC-MS is equipped with a

compact, battery-operated, robust, and field-usable sampling accessory, this latter was not used in this study because PAH measurements were made in road gravel samples [42]. A liquid mixture of 16 PAH at 250 ppb was injected, but the obtained chromatogram showed low intensity peaks for the heavier PAH while the lighter ones seemed to have a higher response factor, suggesting some loss of the heaviest PAH inside the instrument.

Table 5. Comparison with the literature with a focus on methods that had at least one of the two priority characteristics sought, namely portability/transportability or a fully automatic aspect for both sampling and analysis.

Analytical Techniques	Sampling and Preparation	Targeted PAH	Desorption /Injection	Sample Volume	Injected Volume (µL)	Portability	On-line	BaP LOD^{liq} (pg/L)	BaP LOD^{mass} (pg)	BaP LOD^{air} (pg/m^3)	References
Hand-portable HPLC-UV-vis [a]	Syringe for liquid	24 PAH	No	-	5	yes	no	14.1 ± 0.5	-	-	[41]
GC-MS	Syringe for liquid	16 PAH	Thermal (290 °C)	-	20	yes	no	<250,000	-	-	[42]
HPLC-FLD	monolith-based in-tube solid phase microextraction	10 PAH	Chemical (ACN)	6 mL (water)	0.1	no	yes	30			[27]
TD/GC-MS	Adsorption/desorption	-	Thermal	-	-	no	yes	-	-	<540 [b]	[28]
UHPLC-FLD	Offline Chemical desorption [c]	16 US EPA	-	1–72 L (air)	2	no	No [c]	13,000	0.026	903–65,000	This work
				150,000 L (air)			No [d]	13,000	0.026	0.09	
TD/GC-FID	Adsorbent trap at room temperature	18 PAH	Thermal (350 °C)	1–72 L (air)	-	yes	yes	-	29	403–29,000	This work

[a] Deconvolution of overlapping peaks and a pulsed Xenon light source (Ocean Optics, UK); [b] The PAH considered for the LOD is not specified. [c] A solvent volume of 5 mL is required for the possible automatic elution for online analysis. [d] A final solvent volume of 1 mL and a sampling volume of 150 m^3 of air according to a previous study [24].

Regarding the automatic instruments, Pang et al. (2018) have developed an automated and sensitive benchtop device consisting of monolith-based in-tube solid-phase microextraction (IT-SPME) coupled with HPLC-FLD for PAH quantification in water in the range 0.11–5000 ng/L [27]. This type of instrument could be adapted to air analysis, considering the suggestions made in Section 4.2. related to the air sampling, the solvent elution, and the subsequent HPLC analysis.

Furthermore, some authors have reported the high-performance analysis of PAH in the air by thermal desorption (TD) coupled to GC-MS, enabling the continuous measurement of gaseous PAH with a LOD of 540 pg/m^3 [28]. It should be noted that the volume sampled and the sampling rate are not related. However, these two latter instruments remain non-portable for easy and fast in situ measurements.

Finally, of all the above-mentioned devices, none combines the following two characteristics for PAH monitoring: transportability and continuous operation for environmental sample analysis. Table 5 shows that the instrument developed here, i.e., the TD/GC-FID, is the only one that is both transportable and capable of continuous operation for monitoring PAH concentration with a minimal time step of 1 h. For BaP, its LOD varies between 403 and 29,000 pg/m^3 for time resolutions of 24 h and 1 h for 72 and 1 L of air sampling, respectively. The lower value of our LOD agrees with that of 540 pg/m^3 for an unknown PAH that is not specified in their document [28]. A fully autonomous HPLC-FLD method with automated desorption conducted with 5 mL of solvent and the same volumes of air sampled as for GC-FID would achieve a detection limit ranging between 903 and 65 000 pg/m^3 for BaP in air. Of course, these LOD values are much higher than those of 0.09 pg/m^3 obtained with an offline method combining air sampling with a large volume sampler (average of

150 m^3 over 4–5 days) [24], the solvent elution, the final preconcentration to 1 mL, and the UHPLC-FLD optimized in this work.

5. Conclusions

This work presents the analytical performance obtained under controlled laboratory conditions of a new transportable GC-FID capable of continuous operation. To the best of our knowledge, it could be the first instrument reported in the literature to be both transportable and continuously operating for air analysis.

With a 1 L air sample (40 mL/min for 25 min), it was possible to quantify PAH concentrations down to 66–207 ng/m^3 in the gas phase by GC-FID. Such sensitivity appears sufficient to quantify PAH in the effluents of industrial chimneys or in their immediate vicinity, where individual PAH concentrations are in the µg/m^3 range. Such a continuous analytical method can be very useful to optimize industrial processes or study pollution control solutions to reduce emissions. For polluted urban atmospheres or heavily trafficked roads, longer sampling times are required. For instance, daily time steps corresponding to 72 L of sampled air would achieve a LOD of 1.33 ng/m^3 for BaP. The results are thus very promising: the range of linearity and sensitivity is compatible with airborne PAH individual concentrations reported in the literature if a sufficient volume of air is sampled.

With the increase from 16 to 18 PAHs regulated in Europe with the addition of benzo(e)pyrene and benzo(j)fluoranthene [7], a method with satisfactory resolution to better separate them from benzo(b)fluoranthene is required. For this, longer GC columns could be tested at the expense of analysis time, and the use of HPLC method development and optimization software could be helpful. To limit the loss of heavy PAH due to adsorption on the walls, adsorbents and GC materials with better thermal conductivity and thermal resistance should be developed and used. To validate this device with field samples and given that the FID detector is universal, a PAH-specific adsorbent will be needed in the future. Alternatively, by keeping the same mixture of adsorbents, which is non-specific for PAH, this same methodology could be used with a mass spectrometer instead of the FID detector. With a GC-MS, a 10-fold increase in sensitivity is expected, which will allow the measurement of concentrations of a few ng/m^3 with 1 L of air and a 1 h time step and down to 0.05 ng/m^3 for BaP with a 24 h time step. To maintain a good temporal resolution of the measurements, several preconcentration systems could be operated in parallel.

As mentioned earlier, PAH are present in both the gas and particulate phases, so it will be interesting in the future to sample PAH in both phases. For this purpose, a filter could be placed upstream of a trap with a mixture of adsorbents, to sample particulate and gaseous PAH, respectively. These two entities can then be desorbed separately to obtain the distribution of PAH between the two phases. However, further development would be needed to remove the particulate matter from the filter to ensure continuous operation.

In addition, one of the obstacles to the development of such devices is the current non-selectivity of sorbents towards PAH. Indeed, air samples are likely to contain a wide variety of organic pollutants, which requires a relatively selective preconcentration system to avoid a multitude of chromatographic peaks when a non-PAH-specific detector such as an FID is used. The development of adsorbents capable of specifically trapping PAH, or at least polyaromatic compounds, would be a promising way of solving this issue. Some work has already been initiated to develop such adsorbents for PAH water depollution [45–48].

Finally, some effort needs to be made to miniaturize the instrument in the future by reducing the size of the GC key elements (preconcentrator, oven, detector, electronics) and the gas consumption and by integrating the small-scale gas generators inside for H_2 and air.

Supplementary Materials: The following supporting information can be downloaded at: https://www.mdpi.com/article/10.3390/chemosensors11090496/s1, Figure S1: Photo of the instrument Airmo C6-C20+ used for the GC-FID method: (a) general view of the instrument in-place and operational, and (b) sideview. Different units of the instrument are highlighted: (1) computer interface; (2) Airmo C6-C20+ unit; (3) mass spectrometer (not used in this application); (4) hydroxychrom—hydrogen generator; and (5) injector; Figure S2: Time events of the GC-FID method; Figure S3: Chromatogram the developed UHPLC-FLD/UV method for the UV detection at 229 nm, obtained with an injection volume of 2 µL and a PAH concentration of 2.52 (BkF) to 51.48 (NAP) µg/L depending on the PAH. Peak 19 corresponds to acenaphthylene (ACY), while peak 18 is naphtalene (NAP); Figure S4: Calibration curves for the 16 US EPA PAH were obtained with the UHPLC-FLD/UV method, using a gradient of ACN: Water from 45: 55 up to 0: 100 as mobile phase, an oven temperature of 30 °C and an injection volume of 2 µL. The dashed line corresponds to the linear regression in the investigated concentration ranges 0.5–100 µg/L, 0.5–10 µg/L and 0.5–5 µg/L, depending on the PAH; Figure S5: Chromatographic peak area versus PAH mass injected at the GC injector of AirmoVOC C6–C20+ instrument (GC-FID method), allowing vaporization of PAH to mimic gas phase concentrations. The dashed line corresponds to the linear regression in the investigated concentration range, i.e., between 0 and 9.91 ng for all the PAH. These PAH masses were obtained by injecting 1 µg/L of a standard PAH mixture solution of 0–9.9 µg/mL. Because of their co-elutions, the pairs BkF + BbF and BaA + CHY were quantified together. The vertical error bars correspond to the standard deviation of the peak area determined from triplicates.

Author Contributions: Conceptualization, J.V.-R., D.B. (Damien Bazin) and S.L.C.; methodology, J.V.-R., D.B. (Damien Bazin), A.B. and S.L.C.; validation, J.V.-R., A.B., D.B. (Damien Bazin) and S.L.C.; formal analysis, J.V.-R., D.B. (Damien Bourgain) and A.B.; investigation, J.V.-R., D.B. (Damien Bazin), M.M., A.B. and S.L.C.; resources, D.B. (Damien Bazin), S.B.-C. and S.L.C.; writing—original draft preparation, J.V.-R., A.B. and S.L.C.; writing—review and editing, J.V.-R., M.M., A.B., A.G., S.B.-C., D.B. (Damien Bazin) and S.L.C.; visualization, J.V.-R., A.G., M.M., D.B. (Damien Bourgain) and A.B.; supervision, D.B. (Damien Bazin), S.B.-C. and S.L.C.; project administration, D.B. (Damien Bazin), F.A., S.B.-C. and S.L.C.; funding acquisition, D.B. (Damien Bazin), F.A., S.B.-C. and S.L.C. All authors have read and agreed to the published version of the manuscript.

Funding: This work has been conducted in the framework of the CAPTALL project funded by the MICA Carnot Institute. This work was also funded by the region GRAND-EST and ANR (ANR-20-GES1-0013) through the FIGHTVIRUS project. This project was also financed by CHROMATOEC's own funds.

Institutional Review Board Statement: Not applicable.

Informed Consent Statement: Not applicable.

Data Availability Statement: The data presented in this study are available upon request from the corresponding authors. The data are not publicly available because the authors want to keep priority for conference presentations.

Acknowledgments: The authors thank the technical department of ICPEES and more particularly Christophe Sutter (Electronic engineer) and Michel Wolf (Assistant Mechanical Engineer) as well as all the administrative staff of ICPEES for their support. The authors would also like to thank the entire staff of the MICA Carnot Institute for the quality of the exchanges and the animation of this network of laboratories as well as the interdisciplinary thematic institute "Hierarchical and functional mate-rials for health, environment and energy" (ITI HiFunMat).

Conflicts of Interest: The authors declare no conflict of interest. The funders had no role in the design of the study; in the collection, analyses, or interpretation of data; in the writing of the manuscript; or in the decision to publish the results.

References

1. Lamichhane, S.; Bal Krishna, K.C.; Sarukkalige, R. Polycyclic Aromatic Hydrocarbons (PAHs) Removal by Sorption: A Review. *Chemosphere* **2016**, *148*, 336–353. [CrossRef]
2. Mojiri, A.; Zhou, J.L.; Ohashi, A.; Ozaki, N.; Kindaichi, T. Comprehensive Review of Polycyclic Aromatic Hydrocarbons in Water Sources, Their Effects and Treatments. *Sci. Total Environ.* **2019**, *696*, 133971. [CrossRef] [PubMed]

3. Kumar, S.; Negi, S.; Maiti, P. Biological and Analytical Techniques Used for Detection of Polyaromatic Hydrocarbons. *Environ. Sci. Pollut. Res.* **2017**, *24*, 25810–25827. [CrossRef]
4. Fromme, H.; Lahrz, T.; Piloty, M.; Gebhardt, H.; Oddoy, A.; Rüden, H. Polycyclic Aromatic Hydrocarbons inside and Outside of Apartments in an Urban Area. *Sci. Total Environ.* **2004**, *326*, 143–149. [CrossRef]
5. Zhang, L.; Yang, L.; Zhou, Q.; Zhang, X.; Xing, W.; Wei, Y.; Hu, M.; Zhao, L.; Toriba, A.; Hayakawa, K.; et al. Size Distribution of Particulate Polycyclic Aromatic Hydrocarbons in Fresh Combustion Smoke and Ambient Air: A Review. *J. Environ. Sci.* **2020**, *88*, 370–384. [CrossRef]
6. Song, X.; Li, J.; Xu, S.; Ying, R.; Ma, J.; Liao, C.; Liu, D.; Yu, J.; Chen, L. Determination of 16 Polycyclic Aromatic Hydrocarbons in Seawater Using Molecularly Imprinted Solid-Phase Extraction Coupled with Gas Chromatography-Mass Spectrometry. *Talanta* **2012**, *99*, 75–82. [CrossRef]
7. Sommerfeld, T.; Jung, C.; Riedel, J.; Mauch, T.; Sauer, A.; Koch, M. Development of a Certified Reference Material for the Determination of Polycyclic Aromatic Hydrocarbons (PAHs) in Rubber Toy. *Anal. Bioanal. Chem.* **2022**, *414*, 4369–4378. [CrossRef] [PubMed]
8. European Commission. Directive 2004/107/EC of the European Parliament and of the Council of 15 December 2004 Relating to Arsenic, Cadmium, Mercury, Nickel and Polycyclic Aromatic Hydrocarbons in Ambient Air. *Off. J. Eur. Union* **2005**, *26*, 3–16.
9. Chimjarn, S.; Delhomme, O.; Millet, M. Temporal Distribution and Gas/Particle Partitioning of Polycyclic Aromatic Hydrocarbons (PAHs) in the Atmosphere of Strasbourg, France. *Atmosphere* **2021**, *12*, 337. [CrossRef]
10. Bi, X.; Sheng, G.; Peng, P.; Chen, Y.; Zhang, Z.; Fu, J. Distribution of Particulate- and Vapor-Phase n-Alkanes and Polycyclic Aromatic Hydrocarbons in Urban Atmosphere of Guangzhou, China. *Atmos. Environ.* **2003**, *37*, 289–298. [CrossRef]
11. Park, S.S.; Kim, Y.J.; Kang, C.H. Atmospheric Polycyclic Aromatic Hydrocarbons in Seoul, Korea. *Atmos. Environ.* **2002**, *36*, 2917–2924. [CrossRef]
12. Fischer, P.H.; Hoek, G.; van Reeuwijk, H.; Briggs, D.J.; Lebret, E.; van Wijnen, J.H.; Kingham, S.; Elliott, P.E. Traffic-Related Differences in Outdoor and Indoor Concentrations of Particles and Volatile Organic Compounds in Amsterdam. *Atmos. Environ.* **2000**, *34*, 3713–3722. [CrossRef]
13. Delgado-Saborit, J.M.; Stark, C.; Harrison, R.M. Carcinogenic Potential, Levels and Sources of Polycyclic Aromatic Hydrocarbon Mixtures in Indoor and Outdoor Environments and Their Implications for Air Quality Standards. *Environ. Int.* **2011**, *37*, 383–392. [CrossRef]
14. Liaud, C.; Millet, M.; Le Calvé, S. An Analytical Method Coupling Accelerated Solvent Extraction and HPLC-Fluorescence for the Quantification of Particle-Bound PAHs in Indoor Air Sampled with a 3-Stages Cascade Impactor. *Talanta* **2015**, *131*, 386–394. [CrossRef] [PubMed]
15. Palmisani, J.; Di Gilio, A.; Franchini, S.A.; Cotugno, P.; Miniero, D.V.; D'Ambruoso, P.; de Gennaro, G. Particle-Bound PAHs and Elements in a Highly Industrialized City in Southern Italy: PM(2.5) Chemical Characterization and Source Apportionment after the Implementation of Governmental Measures for Air Pollution Mitigation and Control. *Int. J. Environ. Res. Public Health* **2020**, *17*, 4843. [CrossRef] [PubMed]
16. Yang, H.-H.; Lee, W.-J.; Chen, S.-J.; Lai, S.-O. PAH Emission from Various Industrial Stacks. *J. Hazard. Mater.* **1998**, *60*, 159–174. [CrossRef]
17. Li, C.; Mi, H.; Lee, W.; You, W.; Wang, Y. PAH Emission from the Industrial Boilers. *J. Hazard. Mater.* **1999**, *69*, 1–11. [CrossRef]
18. Drabova, L.; Pulkrabova, J.; Kalachova, K.; Tomaniova, M.; Kocourek, V.; Hajslova, J. Rapid Determination of Polycyclic Aromatic Hydrocarbons (PAHs) in Tea Using Two-Dimensional Gas Chromatography Coupled with Time of Flight Mass Spectrometry. *Talanta* **2012**, *100*, 207–216. [CrossRef]
19. Yancheshmeh, R.A.; Bakhtiari, A.R.; Mortazavi, S.; Savabieasfahani, M. Sediment PAH: Contrasting Levels in the Caspian Sea and Anzali Wetland. *Mar. Pollut. Bull.* **2014**, *84*, 391–400. [CrossRef]
20. Guatemala-Morales, G.M.; Beltrán-Medina, E.A.; Murillo-Tovar, M.A.; Ruiz-Palomino, P.; Corona-González, R.I.; Arriola-Guevara, E. Validation of Analytical Conditions for Determination of Polycyclic Aromatic Hydrocarbons in Roasted Coffee by Gas Chromatography–Mass Spectrometry. *Food Chem.* **2016**, *197*, 747–753. [CrossRef]
21. Galmiche, M.; Delhomme, O.; François, Y.-N.; Millet, M. Environmental Analysis of Polar and Non-Polar Polycyclic Aromatic Compounds in Airborne Particulate Matter, Settled Dust and Soot: Part II: Instrumental Analysis and Occurrence. *TrAC Trends in Anal. Chem.* **2021**, *134*, 116146. [CrossRef]
22. Król, S.; Zabiegała, B.; Namieśnik, J. Monitoring and Analytics of Semivolatile Organic Compounds (SVOCs) in Indoor Air. *Anal. Bioanal. Chem.* **2011**, *400*, 1751–1769. [CrossRef] [PubMed]
23. Liaud, C.; Dintzer, T.; Tschamber, V.; Trouve, G.; Le Calvé, S. Particle-Bound PAHs Quantification Using a 3-Stages Cascade Impactor in French Indoor Environments. *Environ. Pollut.* **2014**, *195*, 64–72. [CrossRef] [PubMed]
24. Nursanto, F.R.; Vaz-Ramos, J.; Delhomme, O.; Bégin-Colin, S.; Le Calvé, S. Simultaneous Monitoring of Outdoor PAHs and Particles in a French Peri-Urban Site during COVID Restrictions and the Winter Saharan Dust Event. *Atmosphere* **2022**, *13*, 1435. [CrossRef]
25. Liaud, C.; Chouvenc, S.; Le Calvé, S. Simultaneous Monitoring of Particle-Bound PAHs Inside a Low-Energy School Building and Outdoors over Two Weeks in France. *Atmosphere* **2021**, *12*, 108. [CrossRef]

26. Galmiche, M.; Rodrigues, A.; Motsch, E.; Delhomme, O.; François, Y.-N.; Millet, M. The Use of Pseudo-MRM for a Sensitive and Selective Detection and Quantification of Polycyclic Aromatic Compounds by Tandem Mass Spectrometry. *Rapid Commun. Mass Spectrom.* **2022**, *36*, e9307. [CrossRef]
27. Pang, J.; Yuan, D.; Huang, X. On-Line Combining Monolith-Based in-Tube Solid Phase Microextraction and High-Performance Liquid Chromatography- Fluorescence Detection for the Sensitive Monitoring of Polycyclic Aromatic Hydrocarbons in Complex Samples. *J. Chromatogr. A* **2018**, *1571*, 29–37. [CrossRef]
28. Separation Science in collaboration with Markes International High-Performance Analysis of PAHs in Air by TD–GC–MS. Available online: https://blog.sepscience.com/environmental/high-performance-analysis-of-pahs-in-air-by-td-gc-ms (accessed on 23 February 2023).
29. Knauer Determination of PAH—Method VEV0021J. Available online: https://www.knauer.net/Application/application_notes/short_apps/vev0021j_short_application.pdf (accessed on 29 August 2023).
30. Wasserkort, R.; Hartmann, A.; Widmer, R.M.; Burtscher, H. Correlation between On-Line PAH Detection in Airbone Particle Samples and Their Bacterial Genotoxicity. *Ecotoxicol. Environ. Saf.* **1998**, *40*, 126–136. [CrossRef] [PubMed]
31. Cyr, F.; Tedetti, M.; Besson, F.; Bhairy, N.; Goutx, M. A Glider-Compatible Optical Sensor for the Detection of Polycyclic Aromatic Hydrocarbons in the Marine Environment. *Front. Mar. Sci.* **2019**, *6*. [CrossRef]
32. Alves, C.A.; Vicente, A.M.; Custódio, D.; Cerqueira, M.; Nunes, T.; Pio, C.; Lucarelli, F.; Calzolai, G.; Nava, S.; Diapouli, E.; et al. Polycyclic Aromatic Hydrocarbons and Their Derivatives (Nitro-PAHs, Oxygenated PAHs, and Azaarenes) in PM2.5 from Southern European Cities. *Sci. Total Environ.* **2017**, *595*, 494–504. [CrossRef]
33. Niu, X.; Ho, S.S.H.; Ho, K.F.; Huang, Y.; Sun, J.; Wang, Q.; Zhou, Y.; Zhao, Z.; Cao, J. Atmospheric Levels and Cytotoxicity of Polycyclic Aromatic Hydrocarbons and Oxygenated-PAHs in PM2.5 in the Beijing-Tianjin-Hebei Region. *Environ. Pollut.* **2017**, *231*, 1075–1084. [CrossRef]
34. Li, L.J.; Ho, S.S.H.; Feng, B.; Xu, H.; Wang, T.; Wu, R.; Huang, W.; Qu, L.; Wang, Q.; Cao, J. Characterization of Particulate-Bound Polycyclic Aromatic Compounds (PACs) and Their Oxidations in Heavy Polluted Atmosphere: A Case Study in Urban Beijing, China during Haze Events. *Sci. Total Environ.* **2019**, *660*, 1392–1402. [CrossRef]
35. Zuazagoitia, D.; Millán, E.; Garcia, R. A Screening Method for Polycyclic Aromatic Hydrocarbons Determination in Water by Headspace SPME with GC-FID. *Chromatographia* **2007**, *66*, 773–777. [CrossRef]
36. Carvalho, F.I.M.; Dantas Filho, H.A.; Dantas, K. das G.F. Simultaneous Determination of 16 Polycyclic Aromatic Hydrocarbons in Groundwater by GC-FID after Solid-Phase Extraction. *SN Appl. Sci.* **2019**, *1*, 804. [CrossRef]
37. Gutiérrez-Serpa, A.; Napolitano-Tabares, P.I.; Pino, V.; Jiménez-Moreno, F.; Jiménez-Abizanda, A.I. Silver Nanoparticles Supported onto a Stainless Steel Wire for Direct-Immersion Solid-Phase Microextraction of Polycyclic Aromatic Hydrocarbons Prior to Their Determination by GC-FID. *Microchim. Acta* **2018**, *185*, 341. [CrossRef]
38. Ong, R.; Lundstedt, S.; Haglund, P.; Marriott, P. Pressurised Liquid Extraction–Comprehensive Two-Dimensional Gas Chromatography for Fast-Screening of Polycyclic Aromatic Hydrocarbons in Soil. *J. Chromatogr. A* **2003**, *1019*, 221–232. [CrossRef] [PubMed]
39. Boon, Y.H.; Mohamad Zain, N.N.; Mohamad, S.; Osman, H.; Raoov, M. Magnetic Poly(β-Cyclodextrin-Ionic Liquid) Nanocomposites for Micro-Solid Phase Extraction of Selected Polycyclic Aromatic Hydrocarbons in Rice Samples Prior to GC-FID Analysis. *Food Chem.* **2019**, *278*, 322–332. [CrossRef]
40. Atirah Mohd Nazir, N.; Raoov, M.; Mohamad, S. Spent Tea Leaves as an Adsorbent for Micro-Solid-Phase Extraction of Polycyclic Aromatic Hydrocarbons (PAHs) from Water and Food Samples Prior to GC-FID Analysis. *Microchem. J.* **2020**, *159*, 105581. [CrossRef]
41. Chatzimichail, S.; Rahimi, F.; Saifuddin, A.; Surman, A.J.; Taylor-Robinson, S.D.; Salehi-Reyhani, A. Hand-Portable HPLC with Broadband Spectral Detection Enables Analysis of Complex Polycyclic Aromatic Hydrocarbon Mixtures. *Commun. Chem.* **2021**, *4*, 17. [CrossRef]
42. Thomas, R.; Lee, E.; Truong, T.; Porter, N. The Applicability of Field-Portable GC–MS for the Rapid Sampling and Measurement of High-Boiling-Point Semivolatile Organic Compounds in Environmental Samples. *Spectrocopy* **2016**, *14*, 20–26. Available online: https://www.spectroscopyonline.com/view/applicability-field-portable-gc-ms-rapid-sampling-and-measurement-high-boiling-semivolatile-organic (accessed on 23 February 2023).
43. Robert Owen, B., III. Uses of Portable Gas Chromatography Mass Spectrometers. In *Novel Aspects in Gas Chromatography and Chemometrics*; Moldoveanu, D.S.C., David, P.V., Hoang, A.P.V.D., Eds.; IntechOpen: Rijeka, Croatia, 2022.
44. Truong, T.; Sadowski, C.; Porter, N.; Rands, A.; Richter, B.; Brande, T.; Later, D.; Lee, M. Trace Analysis in the Field Using Gas Chromatography-Mass Spectrometry. *Sci. Chromatogr.* **2014**, *6*, 13–26. [CrossRef]
45. Vaz-Ramos, J.; Bégin, D.; Duenas-Ramirez, P.; Becker, A.; Galmiche, M.; Millet, M.; Bégin-Colin, S.; Calvé, S.L. Magnetic Few-Layer Graphene Nanocomposites for the Highly Efficient Removal of Benzo(a)Pyrene from Water. *Environ. Sci. Nano* **2023**. [CrossRef]
46. Zhang, J.; Li, R.; Ding, G.; Wang, Y.; Wang, C. Sorptive Removal of Phenanthrene from Water by Magnetic Carbon Nanomaterials. *J. Mol. Liq.* **2019**, *293*, 111540. [CrossRef]

47. Pang, L.; Zhang, W.; Zhang, W.; Chen, P.; Yu, J.; Zhu, G.-T.; Zhu, S. Magnetic Graphene Solid-Phase Extraction in the Determination of Polycyclic Aromatic Hydrocarbons in Water. *RSC Adv.* **2017**, *7*, 53720–53727. [CrossRef]
48. Adeola, A.O.; Forbes, P.B.C. Assessment of Reusable Graphene Wool Adsorbent for the Simultaneous Removal of Selected 2–6 Ringed Polycyclic Aromatic Hydrocarbons from Aqueous Solution. *Environ. Technol.* **2020**, 1255–1268. [CrossRef] [PubMed]

Disclaimer/Publisher's Note: The statements, opinions and data contained in all publications are solely those of the individual author(s) and contributor(s) and not of MDPI and/or the editor(s). MDPI and/or the editor(s) disclaim responsibility for any injury to people or property resulting from any ideas, methods, instructions or products referred to in the content.